

A Multiwire Proportional Counter  
For Very High Counting Rates

A. F. Barbosa<sup>\*</sup>, G. P. Guedes

Centro Brasileiro de Pesquisas Físicas - CBPF/CNPq  
Rua Dr. Xavier Sigaud, 150, CEP 22290-180, Rio de Janeiro/RJ, Brazil

E. Tamura

Laboratório Nacional de Luz Síncrotron - LNLS  
Caixa Postal 6192, CEP 13083-970, Campinas/SP, Brazil

I. M. Pepe, N. B. Oliveira

Universidade Federal da Bahia - UFBA  
Instituto de Física, Campus de Ondina, CEP 40210-340, Salvador/BA, Brazil

Preliminary measurements in a proportional counter with two independently counting wires showed that counting rates up to  $10^6$  counts/s per wire can be reached without critical loss in the 'true *versus* measured' linearity relation. Results obtained with a detector containing 30 active wires (2 mm pitch) are presented. To each wire is associated a fast pre-amplifier and a discriminator channel. Global counting rates in excess to  $10^7$  events/s are reported. Data acquisition systems are described for 1D (real time) and 2D (off-line) position sensitive detection systems.

**Key-words:** MWPC, x-ray detector, high counting rate, dead-time.

---

<sup>\*</sup> e-mail: laudo@cat.cbpf.br

## 1. Introduction

The availability of high intensity x-ray sources, specially synchrotron radiation sources, has established the need for the development of high counting rate detectors. Although integrating detectors can cope with high counting rates, some of their features (eg. intrinsic noise, low sensitivity to small intensity variations and to the energy of detected particles) often limit their applicability. Recent developments on avalanche photodiode detectors have resulted in photon counting devices with a dynamic range extending from  $10^{-2}$  to  $10^7$  counts/s (Kishimoto, 1995, Toellner et al., 1994). This is due to the combination of a solid state detecting medium with relatively high avalanche gain (Farrell et al., 1994). However these are low size detectors, with usually less than  $1 \text{ cm}^2$  active surface, and may not easily replace large area detectors. Silicon (Pullia et al., 1995) and plastic scintillator (Radtke, 1990) detectors have also been announced for counting rates above  $10^6$  counts/s.

In the field of gas detectors, it is known that the space charge resulting from exposure to high fluxes ultimately limits their counting rate capability by reducing the electric field in the active region. Some issues have been addressed to bypass this limitation, essentially based in the reduction of the drift path for electrons and ions: microstrip (Oed, 1988), microgap (Hall et al., 1995) and microdot (Biagi et al., 1995) detectors. Very high counting rates may be obtained in a MWPC by appropriate choice of geometry parameters, gas filling, and signal processing electronics (J. Fischer et al., 1985, J. Fischer et al., 1986). The work here presented illustrates the fact that a MWPC could handle relatively high counting rates even in moderate operating conditions. We show results of such a MWPC under high counting rates, that indicate its applicability as a beam monitor or large area detector.

## 2. Detector

In a prototype detector with two wires, we have observed that each wire can reach counting rates up to  $10^6$  counts/s without critical dead-time losses. The counting rate capability of a MWPC could therefore be extended well above  $10^6$  counts/s as long as the wires operate independently. The saturation counting rate depends on the detector geometry, mainly the wire pitch and the anode to cathode gap. But if the wires operate as parallel counters a compromise could be found that sets the counting limit to an acceptable level for a given application. In order to evaluate this possibility, we have built a detector with 33 wires, 4 of which are guard wires and 29 are active counters. The wire plane lies in-between two cathode planes. The wire pitch is 2 mm, and the gap from anode wire plane to cathode planes is 3.2 mm. The detecting area is  $6 \times 6 \text{ cm}^2$  and the active wires diameter is  $20 \text{ }\mu\text{m}$ .

Anode wires are set to high voltage relative to cathode planes, and avalanche signals are capacitively decoupled and connected to a voltage pre-amplifier (Fig. 1). The 'RC' product defining the pre-amplifiers time shaping constant is lower than the inverse of the expected counting rate ( $RC \approx 200 \text{ ns}$ ). A leading-edge discriminator provides a logic signal for each detected photon.

One of the cathode planes is a  $300 \text{ }\mu\text{m}$  carbon-fiber window through which x-ray photons enter the detecting region. For the results shown in the next section the operating gas was Ar + 10%  $\text{CH}_4$ , 0.2 Atm above normal pressure.

### 3. Results

The detector stability, linearity and dynamic range have been characterized with the direct beam of a Cu target x-ray generator, filtered and attenuated with Ni sheets. An  $^{55}\text{Fe}$  source has also been used for stability measurements. In order to check the spatial resolution, the beam profile of the XAFS beam line at LNLS has been scanned.

#### 3.1 Stability

By illuminating the detector with an  $^{55}\text{Fe}$  source and varying the distance from the source to the detector, it has been checked that the detection system was stable for counting rates up to  $10^5$  counts/s per wire. For higher rates -  $10^6$  counts/s per wire - the x-ray generator was used and the output counting rate of a wire was verified to remain stable, within 0.15% of the average, for more than the time taken to carry out other characterization measurements ( $> 1$  hour).

#### 3.2 Linearity

The linearity relation between the true and the measured counting rates has been evaluated by conveniently attenuating the x-ray beam, so that a range of  $10^3$  to  $10^6$  counts/s per wire has been covered. Sub-divisions of this range have been accessed by regularly varying the x-ray tube current.

Counting rate measurements from one central wire are plotted in Fig. 2. It is clear from the figure that dead-time losses are important above  $\approx 10^5$  counts/s. However, since the wires are independent parallel counters, the detection system as a whole is able to process a much higher counting rate. By assuming that the true rate of photons incident to the wire is linearly proportional to the x-ray tube current (and zero at zero current), we have estimated the true counting rate from the measured data

by supposing a non-paralyzable behaviour for the dead time losses (see Section IV). This estimation has only been possible for the first three sets of data in Fig. 2, since no simple mathematical model was applicable for measured counting rates above  $10^6$  counts/s. Fig. 3 illustrates the true *versus* measured counting rate behaviour up to this rate. The best linearity between x-ray tube current and estimated true counting rate has been obtained with 715 ns dead-time value.

In Fig. 4 the beam intensity profile is showed as a function of the x-ray tube current. As the beam intensity increases, deviations from the linear behaviour are clearly seen, since individual wires do not stand counting rates in excess to  $10^6$  counts/s. On the other hand, overall counting rates above  $2 \times 10^7$  counts/s were measured at 37.5 mA x-ray tube current. Corrections to the recorded data are discussed in Section 4.

### 3.3 Dynamic range

The lowest measured counting rate was about 0.8 counts/s per wire, corresponding to cosmic background radiation. As showed in the previous section, saturation counting rate is about  $10^6$  counts/s per wire, which implies a higher limit of  $\approx 3 \times 10^7$  counts/s for the whole detector.

### 3.4 Spatial resolution

With the wires operating independently, the detector may be considered as position sensitive to one dimension. The spatial resolution is in this case determined by the wire pitch (2 mm). Fig. 5 shows the beam intensity profile of the LNLS XAFS beam line in the vertical direction. The beam width in this direction was known to be 1 mm. The beam was monochromatised to 6.5 KeV and attenuated by Ti sheets. As

expected, the profile in Fig. 5 indicates a maximum counting rate in one of the wires, while the other wires detect scattered radiation.

#### 4. Correction for dead-time losses

We have attempted to correct the data shown in Fig. 4 for dead-time losses. A calibration of the true counting rate incident to each wire was needed, and for this purpose we have assumed that the detection system response is linear for low counting rates ( $10^3$  to  $10^4$  counts/s per wire). This is a reasonable assumption, as confirmed by data in Fig. 2. By taking a set of data for one of the wires in which the counting rate ranges from  $10^4$  to  $10^5$  counts/s, it has been possible to estimate the detection system's dead-time. Three mathematical models have been used (Knoll, 1989):

$$y_{np} = \frac{x}{1 + x\tau}; \text{ (non - paralyzable)}$$

$$y_{lr} = x(1 - x\tau); \text{ (low rate)}$$

$$y_p = x\text{Exp}(-x\tau); \text{ (paralyzable)}$$

where  $y$  and  $x$  stand respectively for the measured and the true counting rates, and  $\tau$  is the dead-time. The low rate model function is the one to which both the paralyzable and non-paralyzable functions tend to when the counting rate is very low ( $\ll 1/\tau$ ). Fitting these functions to the set of data we have found:

$$\tau_{np} = 835.5 \text{ ns}$$

$$\tau_{lr} = 758.8 \text{ ns}$$

$$\tau_p = 796.5 \text{ ns}$$

These values are higher than the one obtained in Section 3.2, and may be attributed to the fact that in the present case the x-ray beam is distributed over the whole detector instead of a single wire .

The last two plots in Fig. 2 suggest that, at  $\approx 10^6$  counts/s per wire, the detection system behaviour is closer to a non-paralyzable model, since the measured counting rate does not decrease as it would be expected in a paralyzable model. By inverting  $y_{np}$  it has been possible to correct the whole data set. Assuming that the true counting rate varies linearly with the x-ray tube current, the correction should provide straight lines ( $y = x$ ) when applied to the measured counting rate. Fig 6 shows corrected data obtained for  $\tau = 830.6$  ns.

## 5. Data acquisition system

A complete data acquisition system for the detector includes a pre-amplifier, a discriminator and a counter for each of the active wires. A control unit must also be provided for assembling the information of the whole detector and storing data in memory. Such a system is presently under development at LNLS. The analog part will be composed by pre-amplifiers and discriminators already developed. These shall be upgraded to provide faster signals ( $< 100$  ns duration) and consequently higher counting rates. The counters and the control unit will be implemented in NIM standard modules. Use of Field Programmable Gate Array (FPGA) logic allows packing of up to 30 counters per module. The control unit communicates with each module - *via* a private bus - and with an IBM-PC compatible microcomputer that displays data in real time. A complete description of the system will be presented in the near future.

Two-dimensional position sensitive detectors and the associated data acquisition systems have been prepared for use in a high energy physics experiment at Fermilab/USA (Anjos et al., 1997). In this case, two orthogonal cathode wire planes are included in the detector for sampling the avalanche signals in the X and Y directions. Signals from anode and cathode wires are treated and sent to a controlling

unit that latches the state of all the wires whenever a master gate signal triggers an event (namely charm photoproduction). The latched data is registered in memory and off-line processed by an image reconstruction algorithm.

## **VI Conclusion**

The detector here presented is a MWPC in which the wires have been used as independent photon counters. Although the saturation counting rate for each wire is limited to about  $10^6$  counts/s, the detector as a whole has been able to process  $\approx 3 \times 10^7$  counts/s. It must be noted that the detection system dead-time includes contributions from the pre-amplifiers and from the discriminators output signal width. The limit in counts/s per wire is due to the space charge effect (G. C. Smith, E. Mathieson, 1987), and also to the fact that the used readout electronics is relatively slow, implying dead-time losses. As mentioned in Section V, the pre-amplifier and the discriminator circuits shall be upgraded in the data acquisition system under development. In order to cope with higher counting rates, the detector geometry might be improved (lower anode-to-cathode gap), and a more appropriate gas filling could be used. Counting rates close to  $10^7$  counts/s per wire have been reported (J. Fischer et al., 1985). Dead-time losses have been corrected for, by use of simple mathematical modelling functions. The complete detection system may be used in high counting rate applications requiring 1D and 2D position sensitivity.

## **VII Acknowledgments**

The development of the detector here presented has been supported by the LNS and CBPF directories. The construction of the detector and data acquisition



system has been possible thanks to financial support by PADCT/CNPq and FAPESP (brazilian research funding agencies).

## REFERENCES

- Kishimoto, S. (1995). *Rev. Sci. Instrum.* 66 (2). 2314-2316.
- Toellner, T. S. et al. (1994). *Nucl. Instrum. and Meth. A* 350. 595-600.
- Farrell, R. et al. (1994). *Nucl. Instrum and Meth. A* 353. 176-179.
- Pullia, A et al. (1995). *IEEE Trans. in Nucl. Sci.* 42, 4. 585-589.
- Radtke, J. (1990). Siemens Analytical X-Ray Instruments, Inc. Technical note 322.
- Oed A. (1988). *Nucl. Instrum. and Meth. A* 263. 351.
- Hall, C. J. et al. (1995). *Nucl. Phys. B (Proc. Suppl.)*, 44. 242-245.
- Biagi, S. F. et al. (1995). *Nucl. Instrum and Meth. A* 366. 76-78.
- J. Fischer et al. (1985). *Nucl. Instrum. and Meth. A*238. 249-264.
- J. Fischer et al (1986). *Nucl. Instrum. and Meth. A*246. 511-516.
- G. C. Smith, E. Mathieson (1987). *IEEE Transac. on Nucl. Sc.* NS-34. 410-413.
- Knoll, G. F. (1989). *Radiation Detection and Measurement*. Second Edition. John Wiley & Sons. New York, Chichester, Brisbane, Toronto, Singapore.
- Anjos, J. C. et al. (1997). *Proceedings of the "First Latin American Symposium on High Energy Physics"*. Juan Carlos D'Olivo & Martin Klein Editors, American Institute of Physics.

## Figure Captions

Fig. 1: Schematic view of the detector, illustrating the connection of the wires to the pre-amplifiers and to the high voltage supply.

Fig. 2: Plots of the linearity measurements for one wire, with counting rates extending from  $10^3$  to  $10^6$  counts/s.

Fig. 3: True *versus* measured counting rate relation for one wire, estimated from the first three sets of data in Fig. 2 by use of a non-paralyzable dead-time model function.

Fig. 4: Beam intensity profile as a function of the x-ray tube current.

Fig. 5: Attenuated synchrotron radiation beam intensity profile, obtained at the XAFS beam line of the LNLS.

Fig. 6: Correction to data in Fig. 4, obtained from a non-paralyzable mathematical model with  $\tau = 830.6$  ns.

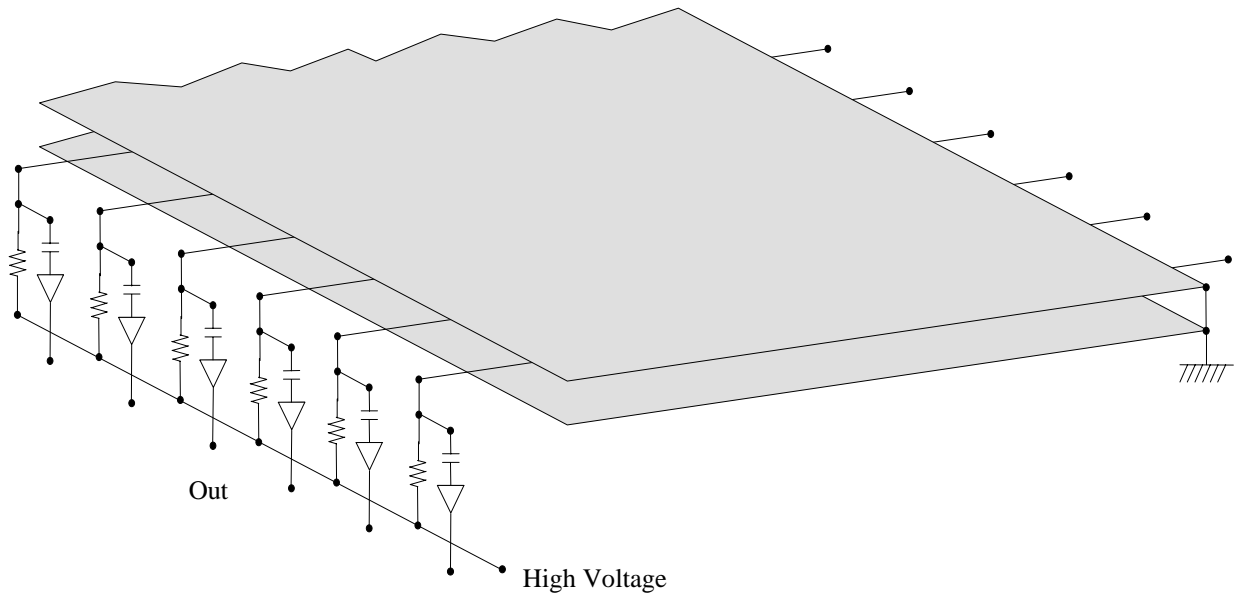


Fig. 1: Schematic view of the detector, illustrating the connection of the wires to the pre-amplifiers and to the high voltage supply.

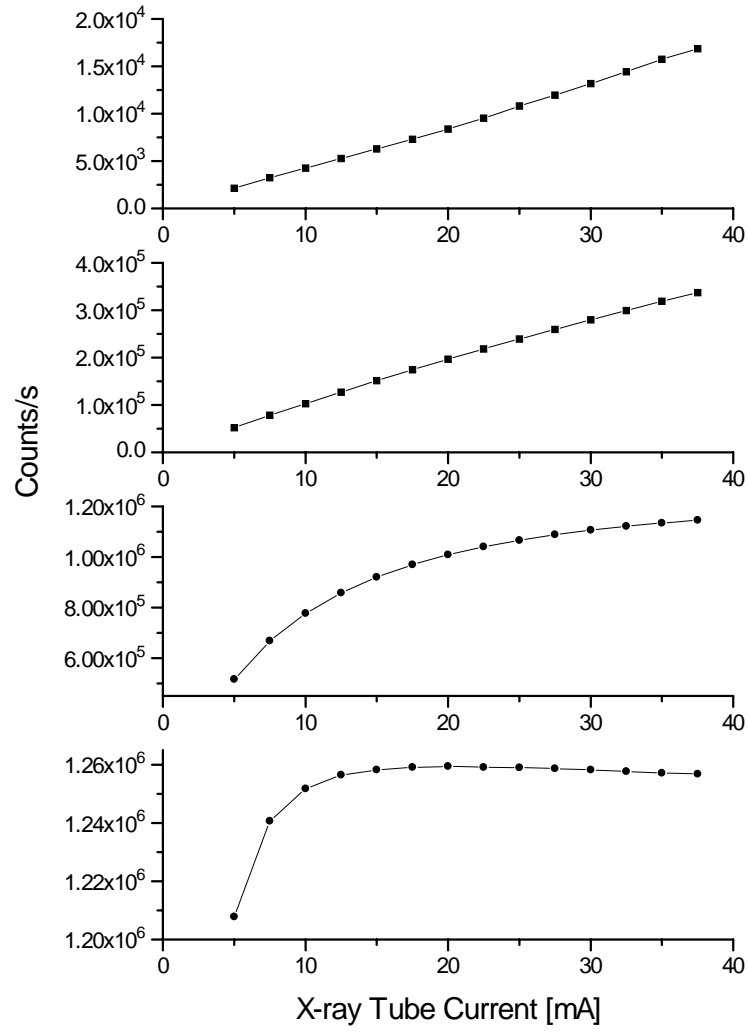


Fig. 2: Plots of the linearity measurements for one wire, with counting rates extending from 10<sup>3</sup> to 10<sup>6</sup> counts/s.

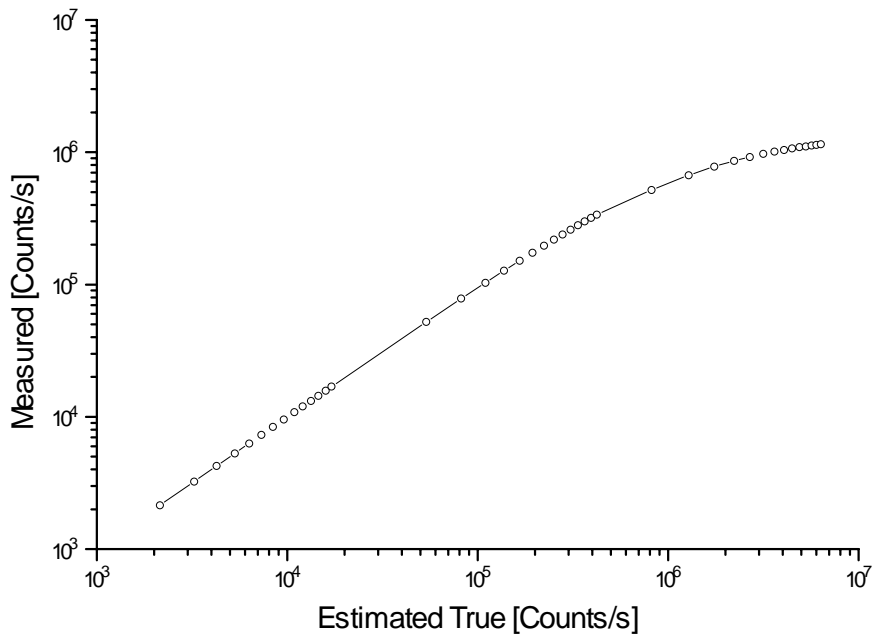


Fig. 3: True *versus* measured counting rate relation for one wire, estimated from the first three sets of data in Fig. 2 by use of a non-paralyzable dead-time model function.

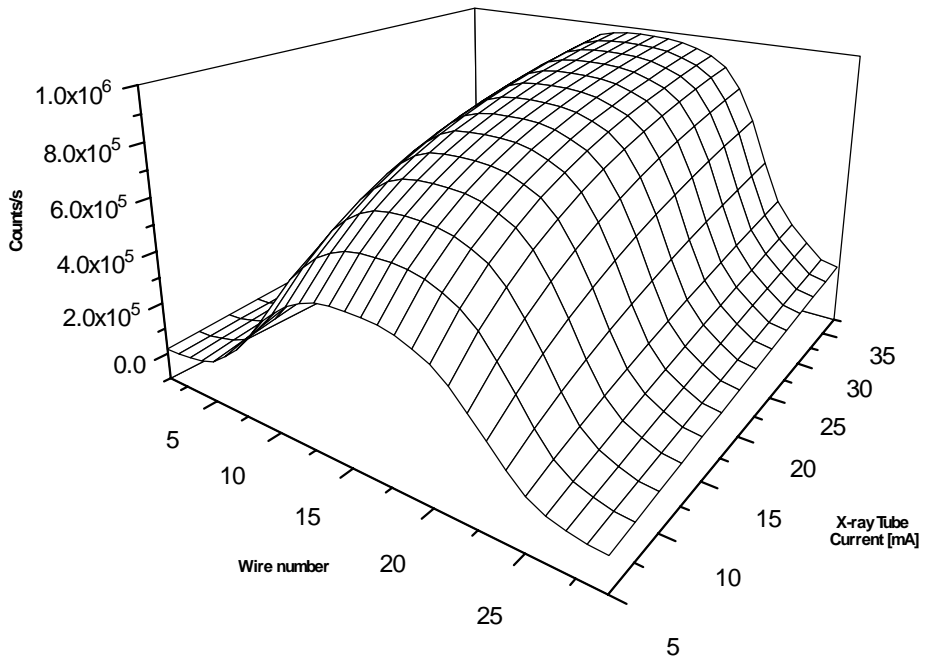


Fig. 4: Beam intensity profile as a function of the x-ray tube current.

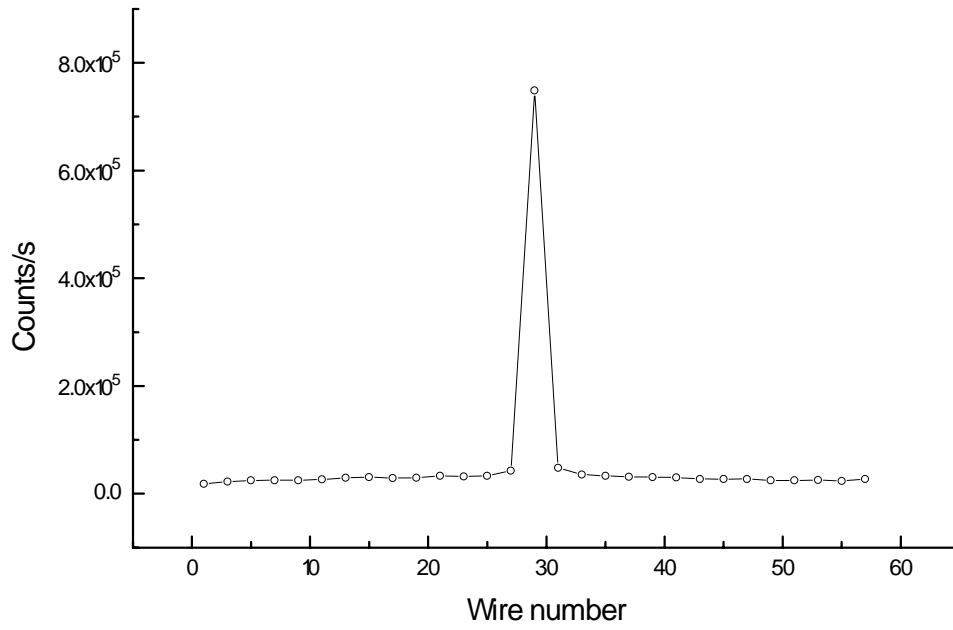


Fig. 5: Attenuated synchrotron radiation beam intensity profile, obtained at the XAFS beam line of the LNLS.



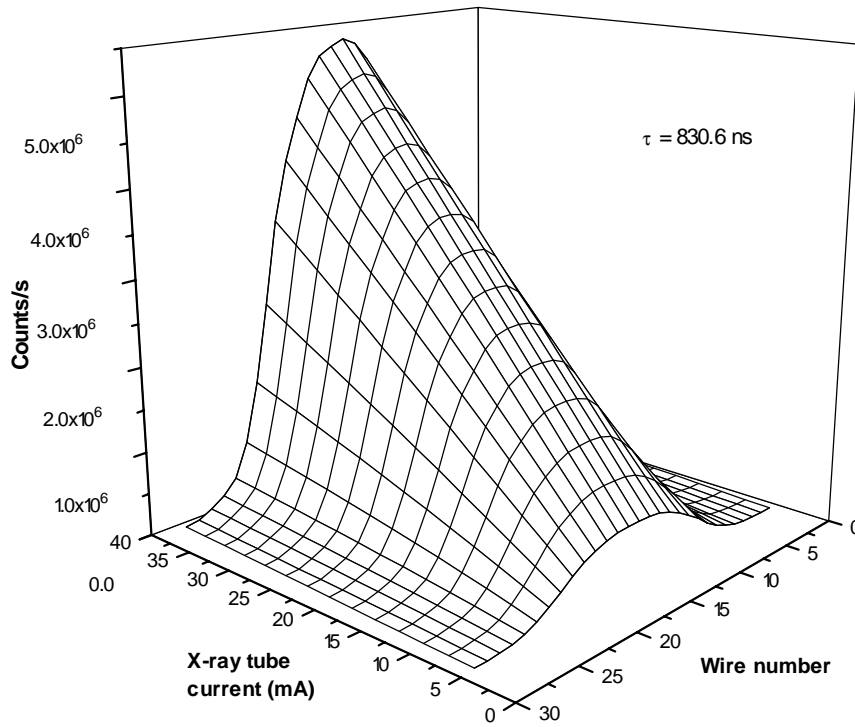


Fig. 6: Correction to data in Fig. 4, obtained from a non-paralyzable mathematical model with  $\tau = 830.6 \text{ ns}$ .